Deep level photothermal spectroscopy: Physical principles and applications to semi-insulating GaAs band-gap multiple trap states

Andreas Mandelis[a] and Jun Xia
Center for Advanced Diffusion-Wave Technologies (CADIFT), Department of Mechanical and Industrial Engineering, University of Toronto, Toronto, Ontario M5S 3G8, Canada

A coupled transport-rate theory of free photoexcited carrier densities and band-gap trap states in direct-gap semiconductors with fast band-to-band recombination rates is presented. The rate equations are decoupled and solved analytically by means of an adiabatic principle which leads to time gating of photothermal emission and capture transport processes between trap states and bandedges occurring with time constants much longer than the recombination lifetime. This theory exploits the adiabatic character of photoexcitation of nonequilibrium excess free carriers which attains steady-state distribution at times very short compared to trap emission and capture effects induced by thermal transport to and from the bandedges of the semiconductor. The theory accounts for the absorption of a sub-band-gap probe laser beam by free carriers (both electrons and holes) photogenerated by a super-band-gap laser beam, as well as absorption by nonequilibrium trapped carriers in the band-gap states due to thermal emission and capture events. The theory forms the basis of a new two-laser-beam deep level photothermal spectroscopy (DLPTS). The latter was implemented and tested on semi-insulating (SI)-GaAs. DLPTS and photocarrier radiometric signals were used to validate the theory. The generated experimental temperature-scanned photothermal spectra and time-resolved transients were fitted with the multiple-trap theory and yielded superpositions of energy levels and capture cross sections. It was found that the one-trap theory commonly used in conventional deep level transient spectroscopy based techniques, such as photoinduced transient spectroscopy, does not give a good fit to the experimental DLPTS spectrum. The methodology encompassing the adiabatic theory and combined DLPTS time-scanned transients and temperature-scanned spectra amounts to an analytical quantitative photothermal spectroscopy capable of noncontact all-optical probing of band-gap defect/impurity state energy distributions and capture cross sections in direct-gap semiconductors, and SI-GaAs in particular. © *2008 American Institute of Physics*. [DOI: 10.1063/1.2842401]

I. INTRODUCTION

Deep level transient spectroscopy (DLTS), first introduced by Lang,[1] is a powerful tool for detection and characterization of deep level generating defects in semiconductors. Conventional DLTS requires a depleted region at the semiconductor surface and measures the capacitance change after an electrical or optical pulse. This method, however, cannot be applied to high-resistivity materials, since the Debye–Huckel length is too large (several millimeters for semi-insulating GaAs at 300 K) and typically exceeds sample dimensions.[2] An alternative technique, known as photoinduced transient spectroscopy (PITS),[3,4] has been developed by measuring the photocurrent transient in the sample. Other photoconductivity-based spectroscopic methods have also been developed to obtain density of states (DOS) within the band gap of photoconductive crystalline and disordered semiconductors.[5–9] PITS and related photoconductivity methods do not require the preparation of *p-n* junctions, but an electrical contact is still needed which may introduce nonlinear effects and energy-band distortions at the interface. In addition to the intrinsic errors that may be induced, this contact renders the technique intrusive and hence not practicable

for the direct probing of materials for integrated circuit (IC) processes. Any spectroscopic measurements of DOS may also be compromised.

During the past few years, several noncontact techniques have been developed for the determination of the position of discrete states in the band gap;[10–13] however, these techniques tend to be quite restrictive in their application scope. For instance, laser-microwave deep level transient spectroscopy (LM-DLTS) requires, for detection, the presence of free-carrier concentrations within limits determined to be[11] $8.3 \times 10^{10} \leq n \leq 2.6 \times 10^{13}$ cm^{-3}. Furthermore, the spatial resolution of LM-DLTS is limited by the microwave probe-beam spot size (on the order of 10–20 mm).

In an earlier paper, we introduced an all optical deep level photothermal spectroscopy (DLPTS),[14] which utilizes a sub-band-gap laser to monitor the concentration of free carriers and the density of occupied states resulting from photoexcitation by a modulated coincident super-band-gap laser beam. The technique was applied to semi-insulating (SI)-GaAs and a well-defined peak was observed in the temperature-scanned spectrum above room temperature. Based on a single trap-level theory, we identified the peak as corresponding to the EL3 level; however, the simulated spectrum did not fit very well due to the oversimplifications of

---
[a]Electronic mail: mandelis@mie.utoronto.ca.

the theory. In this paper the notion of "level" is purely energetic and is assumed to include one or more electronic quantum energy states specific to an impurity which acts like an electron or hole trap. Therefore, the two terms will be used interchangeably. With a view to the development of DLPTS into a full band-gap DOS spectroscopy, we introduce a comprehensive adiabatic rate theory with discrete coupled multiple energy levels which is subsequently adapted to DLPTS signals, and we provide experimental implementation of the theory in SI-GaAs crystals. Experimentally, two independent methods-embodiments of DLPTS are combined: transient responses to optical pulses (time domain) and rate-window temperature scans (frequency domain). The obtained consistency between experimental data and theoretical/computational fits yields a higher level of reliability in the interpretation of the data in terms of energy-state locations and capture cross sections in the SI-GaAs band gap than conventional semiconductor spectroscopic techniques. Furthermore, the transport rate theory's adiabatic time-gating concept obviates several persistent shortcomings of the current mathematical approaches to trapped-carrier emission and capture rate kinetics.

II. MULTITRAP TRANSPORT-RATE TIME-GATING THEORY

A. Emission and capture rates under optothermal (nonequilibrium) conditions

In time-domain theories of transient optoelectronic effects in semiconductors several not-well-justified approximations have been employed to decouple the transport-rate equations for carriers ejected into the conduction or valence bands, as the case may be, so as to provide analytical solutions to the ensuing (usually) current transient. To date there remain persistent shortcomings of carrier rate theories which prohibit rigorous solutions of the coupled rate equations. Several groups[15,16] considered a single trap in the band gap of GaAs and neglected terms associated with the capture of charge carriers by the occupied electron or hole trap in order to obtain analytical solutions for the free-electron and free-hole densities, $n(t)$ and $p(t)$, respectively, in PITS experiments. Along the same line of thought, Yoshie and Kamiahara[17] presented a PITS analysis of high-resistivity CdS single crystals by assuming the value of the lifetime of free electrons in the single-trap rate equations to be constant. This amounts to a constant term associated with the capture of carriers, an approximation which is not justified, as the lifetime depends on the time-dependent trapped-carrier density. Difficulties with inclusion of capture processes in the rate equations are a long-standing issue impacting the ability of theoretical models to yield information on the numbers and energetic locations of band-gap trap levels responsible for carrier emission to the free bands. The major mathematical problem with carrier capture processes in band-gap traps is that they couple the occupied carrier densities to the generation rate of free carriers in a nonlinear manner. Many researchers have resorted to phenomenological solutions of the rate equations by superposing arbitrary numbers of time-decay exponentials[15] with little or no correspondence to the

underlying physical processes and with the sole purpose of best-fitting experimental data. More elaborate computational models have also been presented taking into account the non-exponential character of photocurrent transient (PITS) signals;[18] however, they have been unable to identify physical mechanisms for the observed transients.

Contrary to the conventional approximations and phenomenological computational schemes, a trapped-carrier transport-rate time-gating concept was developed for the rigorous solution of nonlinearly coupled rate equations in this work. This is an adiabatic principle separating out coupled optical and thermal/kinetic processes. It is capable of providing explicit solutions to multilevel coupled photocarrier emission and capture kinetics for semiconductors which are characterized by fast optical generation and recombination rates well separated temporally from trap-to-bandedge thermal emission rates in the presence of nonequilibrium emission/capture photothermal processes. This is normally the case with photonic direct-gap semiconductors. To avoid unnecessary mathematical complexity, the theory is developed for a discrete two-state trap manifold but can be readily generalized to an arbitrary number of trap states and this has been done in the case of SI-GaAs in the experimental part of the paper. The transport-rate time-gating theory allows for a rigorous solution of the coupled rate equations and includes both emission and capture processes with no further assumptions with regard to the magnitude of contributions of trapped carriers to the free-carrier density.

The classical Shockley–Read approach of equilibrium semiconductor statistics[19] has been extended to nonequilibrium steady-state statistics by Simmons and Taylor.[20] As a first step toward extending these steady-state formalisms to a continuously distributed nonequilibrium, non-steady-state density of states within the band gap, we consider energetically discrete traps which are encountered in several impurity semiconductors, such as in SI-GaAs. For simplicity, two discrete traps at energy levels E_1 and E_2 above the valence band maximum E_V are considered with trap densities N_1 and N_2 and trapped electron densities $n_1(t)$ and $n_2(t)$. The free-electron and free-hole densities are $n(t)$ and $p(t)$, respectively. At absolute temperature T the electron emission and capture probabilities to and from the conduction band are $e_{nj}(T)$ and C_{nj}, $(j=1,2)$. Hole emission and capture probabilities to and from the valence band are $e_{pj}(T)$ and C_{pj}. The free electron and hole recombination lifetimes are τ_n and τ_p, respectively. The band-gap kinetic energy diagram far from the semiconductor surface is shown in Fig. 1 and the rate equations under optical excitation conditions with band-to-band electron and hole generation rates $G(t)_n^{\text{op}}$ and $G(t)_p^{\text{op}}$ can be written as follows:

$$\frac{dn(t)}{dt} = G(t)_n^{\text{op}} + e_{n1}n_1(t) + e_{n2}n_2(t) - C_{n1}n(t)[N_1 - n_1(t)]$$

$$- C_{n2}n(t)[N_2 - n_2(t)] - \frac{n(t)}{\tau_n}, \tag{1a}$$
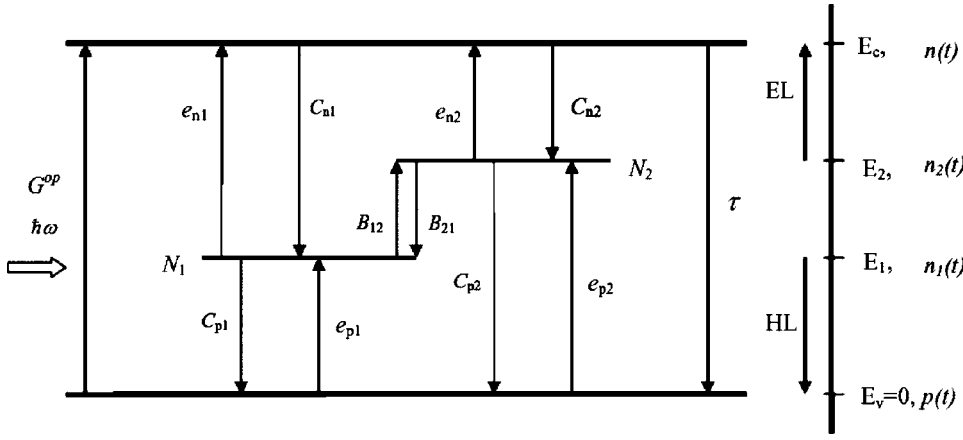
FIG. 1. Energy diagram of a semiconductor band gap with two trap states (E_1, N_1) and (E_2, N_2) with capture and emission-rate processes shown, including the intratrap transport rates B_{ij}. The super-band-gap optical source generation rate is $G(t)^{\text{op}}$, assumed common for both electron and hole photoexcitations.

$$\frac{dn_1(t)}{dt} = -e_{n1}n_1(t) + C_{n1}n(t)[N_1 - n_1(t)] - C_{p1}n_1(t)p(t)$$

$$+ e_{p1}[N_1 - n_1(t)] + B_{21}n_2(t)[N_1 - n_1(t)]$$

$$- B_{12}n_1(t)[N_2 - n_2(t)], \tag{1b}$$

$$\frac{dn_2(t)}{dt} = -e_{n2}n_2(t) + C_{n2}n(t)[N_2 - n_2(t)] - C_{p2}n_2(t)p(t)$$

$$+ e_{p1}[N_2 - n_2(t)] + B_{12}n_1(t)[N_2 - n_2(t)]$$

$$- B_{21}n_2(t)[N_1 - n_1(t)], \tag{1c}$$

$$\frac{dp(t)}{dt} = G(t)_p^{\text{op}} + e_{p1}[N_1 - n_1(t)] + e_{p2}[N_2 - n_2(t)]$$

$$- C_{p1}p(t)n_1(t) - C_{p2}p(t)n_2(t) - \frac{p(t)}{\tau_p}. \tag{1d}$$

In the foregoing coupled rate equations the equilibrium thermal emission rates are defined as follows:

$$e_{n1}(T) = e_{n10}N_C e^{-(E_C - E_1)/k_B T},$$

$$e_{n2}(T) = e_{n20}N_C e^{-(E_C - E_2)/k_B T},$$

$$e_{p1}(T) = e_{p10}N_V e^{-E_1/k_B T}, \tag{2}$$

$$e_{p2}(T) = e_{p20}N_V e^{-E_2/k_B T},$$

$$B_{12}(T) = B_{12}^{(0)} e^{-(E_2 - E_1)/k_B T},$$

where $N_C(T)$ and $N_V(T)$ are the effective densities of states in the conduction and valence bands, respectively.[21] Furthermore, $e_{nj0}(T) = \gamma_{nj}\sigma_{nj}T^2$ and $e_{pj0}(T) = \gamma_{pj}\sigma_{pj}T^2$ where γ_{nj} and γ_{pj} are material constants and σ_{nj} (σ_{pj}) are capture cross sections for electrons (holes) at trap (j). B_{12} and B_{21} are intertrap carrier emission rates. They are the equivalent of Einstein A and B coefficients and act as coupling factors between Eqs. (1b) and (1c). The group of Eq. (2) represents thermal-equilibrium expressions in the absence of external photothermal carrier sources. Under super-band-gap illumination, the probabilities e_{nj} and e_{pj} must be modified to involve optical transition components which drive the semiconductor away from equilibrium. In that case the overall nonequilibrium photothermal emission probabilities become

$$e_{nj,pj}(T) = e_{nj,pj}^{\text{op}} + e_{nj,pj}^{\text{th}}(T), \quad j = 1, 2. \tag{3}$$

Similarly, the overall photothermal carrier generation rates under nonequilibrium conditions are

$$G_{n,p}(t,T) = G(t)_{n,p}^{\text{op}} + G(T)_{n,p}^{\text{th}} \approx G(t)_{n,p}^{\text{op}}, \tag{4}$$

because the thermal generation rates from trap to bandedge are negligible compared to the optical band-to-band generation rates under laser excitation. An additional simplification normally occurs under fast optical generation compared to thermal free-carrier emission, so that equal densities of free electrons and holes are created optically as follows:

$$G_n^{\text{op}} = G_p^{\text{op}} \equiv G^{\text{op}}. \tag{5}$$

When the time constants of the optical and thermal generation rates of free carriers are very different (by at least one order of magnitude), adiabatic transport-rate time gating can be invoked to separate the two processes. In that case the optical process gives rise to a carrier source for the thermal process. Focusing on the free-electron density first, the thermal and optical contributions can be separated as follows:

$$n(t,T) = n_{\text{th}}(t,T) + \Delta n_{\text{op}}(t). \tag{6}$$

The same adiabatic assumption can be applied to Eq. (1a) to separate out optical and thermal components as follows:

$$\frac{dn(t)}{dt} = \frac{dn_{\text{th}}(t,T)}{dt} + \frac{d\Delta n_{\text{op}}(t)}{dt} = \{e_{n1}n_1(t) + e_{n2}n_2(t)$$

$$- C_{n1}n_{\text{th}}(t)[N_1 - n_1(t)] - C_{n2}n_{\text{th}}(t)[N_2 - n_2(t)]\}$$

$$+ \left\{ G(t)^{\text{op}} - C_{n1}\Delta n_{\text{op}}(t)[N_1 - n_1(t)] - C_{n2}\Delta n_{\text{op}}(t) \right.$$

$$\left. \times [N_2 - n_2(t)] - \frac{\Delta n_{\text{op}}(t)}{\tau_n} \right\}. \tag{7}$$

Due to the fast recombination following optical excitation, the electron occupation densities of the traps do not change appreciably thermally within the recombination lifetime τ_n; therefore, for the purposes of estimating the optically generated free-electron density, Eq. (7) yields a (thermally adiabatic) optical rate time-gated equation valid at times $\sim O(\tau_n)$ or earlier as follows:

$$\frac{d\Delta n_{\mathrm{op}}(t)}{dt} + \frac{\Delta n_{\mathrm{op}}(t)}{\tau_{0n}} = \begin{cases} G(t)^{\mathrm{op}}, & 0 < t < t_P, \\ 0, & t > t_P, \end{cases} \qquad (8)$$

where t_P is the duration of the optical generation source and the effective recombination time is defined as

$$\frac{1}{\tau_{0n}} \equiv \frac{1}{\tau_n} + \sum_{j=1}^{2} C_{nj}(N_j - n_{j0}), \quad n_{j0} \equiv n_j(t=0^-). \qquad (9)$$

Here 0^- stands for times before, but infinitesimally close to, $t=0$ when the optical source is turned on. n_{j0} is the initial (equilibrium) occupied fraction of trap N_i before the onset of optical carrier generation. The time constant τ_{0n} represents the full decay time which comprises the band-to-band recombination rate (both radiative, R, and nonradiative, NR, components) as follows:

$$\frac{1}{\tau_n} = \frac{1}{\tau_R} + \frac{1}{\tau_{NR}}, \qquad (10)$$

and the band-to-trap capture rates for both assumed trapping levels. Under the assumption of constant optical fluence during the illumination period $t \ll t_P$, solution of Eq. (8) yields

$$\Delta n_{\mathrm{op}}(t) = G^{\mathrm{op}}\tau_{0n}(1 - e^{-t/\tau_{0n}}) \simeq G^{\mathrm{op}}\tau_{0n}. \qquad (11)$$

Similarly for holes, the adiabatic assumption can be applied to Eq. (1d) to separate optical and thermal components as follows:

$$p(t,T) = p_{\mathrm{th}}(t,T) + \Delta p_{\mathrm{op}}(t) \qquad (12a)$$

leading to the optical generation rate

$$\Delta p_{\mathrm{op}}(t) = G^{\mathrm{op}}\tau_{0p}(1 - e^{-t/\tau_{0p}}) \simeq G^{\mathrm{op}}\tau_{0p}, \qquad (12b)$$

where

$$\frac{1}{\tau_{0p}} \equiv \frac{1}{\tau_p} + \sum_{j=1}^{2} C_{pj}n_{j0}. \qquad (13)$$

Once the optical generation steady state of free electrons has been established within times on the order of τ_{0n}, τ_{0p}, the trap-state carrier densities at times commensurate with thermal emission and capture rates can be described by

$$\frac{dn_1(t)}{dt} = -e_{n1}n_1(t) + C_{n1}[n_s(T) + G^{\mathrm{op}}\tau_{0n}][N_1 - n_1(t)]$$

$$+ e_{p1}[N_1 - n_1(t)] - C_{p1}[p_s(T) + G^{\mathrm{op}}\tau_{0p}]n_1(t)$$

$$+ B_{21}n_2(t)[N_1 - n_1(t)] - B_{12}[N_2 - n_2(t)]n_1(t) \qquad (14a)$$

and

$$\frac{dn_2(t)}{dt} = -e_{n2}n_2(t) + C_{n2}[n_s(T) + G^{\mathrm{op}}\tau_{0n}][N_2 - n_2(t)]$$

$$+ e_{p2}[N_2 - n_2(t)] - C_{p2}[p_s(T) + G^{\mathrm{op}}\tau_{0p}]n_2(t)$$

$$+ B_{12}n_1(t)[N_2 - n_2(t)] - B_{21}[N_1 - n_1(t)]n_2(t). \qquad (14b)$$

Here $n_s(T)$ and $p_s(T)$ are thermal-equilibrium carrier densities. It can be seen that the intertrap level interaction terms B_{12} and B_{21}, Fig. 1, couple the trapped-carrier transport-rate

equations (14a) and (14b) in a nonlinear manner. These interactions can only be significant when the electron quasi-Fermi level lies between the two trap levels in which case the trap populations N_1 and N_2 can be significantly different. Normally, the levels are close enough to each other so that they are under thermal quasiequilibrium conditions and the B_{ij} terms are approximately equal, thus canceling out. This allows Eqs. (14a) and (14b) to become decoupled. If $n_0(T)$ and $p_0(T)$ denote the initial free-carrier densities for the thermal emission and capture processes at times long enough for the optical system to reach steady state, Eqs. (11), (12a), and (12b), yet short enough to represent initial conditions for the thermal system,

$$n_0(T) \equiv n_s(T) + G^{\mathrm{op}}\tau_{0n}, \quad p_0(T) \equiv p_s(T) + G^{\mathrm{op}}\tau_{0p}, \qquad (15)$$

then Eqs. (14a) and (14b) simplify considerably as follows:

$$\frac{dn_1(t)}{dt} + F_1(T)n_1(t) = [C_{n1}n_0(T) + e_{p1}]N_1,$$

$$\frac{dn_2(t)}{dt} + F_2(T)n_1(t) = [C_{n2}n_0(T) + e_{p2}]N_2, \qquad (16)$$

where $F_j(T)$ are total photothermal carrier transport (emission and capture) rates from all band-gap trapped carriers into both conduction and valence bands as follows:

$$F_j(T) \equiv e_{nj}(T) + e_{pj}(T) + C_{nj}n_0(T) + C_{pj}p_0(T), \quad j = 1,2. \qquad (17)$$

At $t=0$, the rate equations (1b) and (1c) yield the initial (equilibrium) values

$$n_{j0} \equiv n_j(0^-) = \left[\frac{C_{nj}n_s(T) + e_{pj}^{\mathrm{th}}(T)}{F_j^{\mathrm{th}}(T)}\right]N_j, \quad j = 1,2. \qquad (18)$$

These are the initial conditions for the optical equations (8) and (9) and $F_j^{\mathrm{th}}(T)$ are total thermal transport rates in the dark, analogous to the nonequilibrium rates $F_j(T)$ as follows:

$$F_j^{\mathrm{th}}(T) \equiv e_{nj}^{\mathrm{th}}(T) + e_{pj}^{\mathrm{th}}(T) + C_{nj}n_s(T) + C_{pj}p_s(T), \quad j = 1,2. \qquad (19)$$

The following definitions of trap occupation probabilities (or fractions) can now be made under nonequilibrium (photothermal) and dark (thermal) conditions, respectively,

$$P_j(T) \equiv \frac{C_{nj}n_0(T) + e_{pj}(T)}{F_j(T)},$$

$$P_j^{\mathrm{th}}(T) \equiv \frac{C_{nj}n_s(T) + e_{pj}^{\mathrm{th}}(T)}{F_j^{\mathrm{th}}(T)}, \qquad j = 1,2. \qquad (20)$$

The carrier transport-rate time-gating theory consists of (i) solving the photothermal rate equation (16) for all trap states for the trapped-carrier evolution following the onset of an optical pulse, and (ii) using the resulting solutions as inputs to the temporal behavior of the relatively slowly thermally ejected and captured carriers at all times during and after the cessation of the illuminating pulse.

B. Electron-density kinetics during optical illumination: $0 \leq t \leq t_P$

The rate equation (16) combined with the initial condition (18) can be solved using standard techniques to yield the time-dependent densities of electronic carriers in the two assumed traps during the band-to-band optical excitation process which generates free carriers filling the traps as follows:

$$n_j(t,T) = N_j[P_j(T) - \Delta P_j(T)\exp(-F_j t)], \quad j = 1,2. \quad (21)$$

$\Delta P_j(T)$ is the nonequilibrium probability gradient

$$\Delta P_j(T) \equiv P_j(T) - P_j^{th}(T), \quad j = 1,2 \quad (22)$$

and it is the measure of the degree of nonequilibrium of the trapped-carrier densities, with the expressions P_j and P_j^{th} given by Eq. (20). $\Delta P_j(T)$ acts as a force driving all nonequilibrium trapped-carrier transport in the semiconductor in order to restore the equilibrium state. From Eq. (15) it can be seen that isothermally increasing the optical excitation rate G^{op} drives the trapped-carrier density farther away from equilibrium, thus increasing $\Delta P_j(T)$. The physical interpretation of Eqs. (21) and (22) can be formulated in terms of the central assumption of the carrier transport-rate time-gating theory that during band-to-band optical excitation the optical steady state within the free bands is attained long before any other time-dependent effects such as interactions with trapped states and thermal emissions from those states. Once the optical steady state and the nonequilibrium probability gradient have been established through photoexcitation and fast band-to-band recombination (essentially instantaneously compared to the nonequilibrium interaction time constant F_j^{-1}), the excess free-carrier densities interact dynamically with the band-gap trap states exchanging carriers as shown in Fig. 1 and perturbing the equilibrium occupation densities. $n_j(t,T)$ represents the temporal buildup of trapped-carrier densities under the initial condition of optical nonequilibrium steady state. Inserting the time-dependent trapped-carrier densities (21) into the rate equation (1a) for the free-electron density $n(t)$ during illumination with the optical pulse yields the inhomogeneous isothermal differential equation

$$\frac{dn(t,T)}{dt} + \left\{ C_{n1}[N_1 - n_1(t,T)] + C_{n2}[N_2 - n_2(t,T)] \right.$$
$$\left. + \frac{1}{\tau_n(T)} \right\} n(t,T)$$
$$= G^{op} + e_{n1}(T)n_1(t,T) + e_{n2}(T)n_2(t,T). \quad (23)$$

It is seen that the adiabatic transport-rate time-gating concept allows for decoupling the rates $dn(t,T)/dt$ and $dn_j(t,T)/dt$ through the prior solution for $n_j(t,T)$, Eq. (21). The general solution of Eq. (23) may be written as

$$n(t) = K_1 \exp\left\{ -\int^t \left[\sum_{i=1}^{2} (C_{ni}[N_i - n_i(t')]) + \tau_n^{-1} \right] dt' \right\}$$
$$+ \exp\left\{ -\int^t \left[\sum_{i=1}^{2} (C_{ni}[N_i - n_i(t')]) + \tau_n^{-1} \right] dt' \right\}$$
$$\times \int^t \exp\left\{ \int^{t'} \left[\sum_{i=1}^{2} (C_{ni}[N_i - n_i(y)]) + \tau_n^{-1} \right] dy \right\}$$
$$\times \left[G^{op} + \sum_{i=1}^{2} e_{ni}n_i(t') \right] dt', \quad (24)$$

where K_1 is an integration constant to be determined via the initial (equilibrium) condition at $t = 0^-$ and the temperature dependence has been suppressed. A nonequilibrium photothermal relaxation lifetime of free electrons into the two trap states can be defined in a form analogous to the thermal-equilibrium effective electron recombination time, Eq. (9),

$$\frac{1}{\tau_{1n}} \equiv \frac{1}{\tau_n} + \sum_{i=1}^{2} C_{ni}N_i[1 - P_i(T)], \quad (25)$$

which allows recasting Eq. (24) in a simpler and compact form

$$n(t) = [K_1 + J_2(t)]e^{-J_1(t)}, \quad (26a)$$

where

$$J_1(t) \equiv \int^t \left[\sum_{i=1}^{2} (C_{ni}[N_i - n_i(t')]) + \tau_n^{-1} \right] dt'$$
$$= \frac{t}{\tau_{1n}} - \sum_{i=1}^{2} A_{ni} \exp(-F_i t) \quad (26b)$$

with the following definition of the nonequilibrium capture to total photothermal transport-rate ratios for electrons from Eqs. (17) and (22):

$$A_{ni}(T) \equiv C_{ni}N_i\left[\frac{\Delta P_i(T)}{F_i(T)} \right], \quad i = 1,2. \quad (26c)$$

$J_2(t)$ represents the integral in the argument of the last exponent of Eq. (24), now written in the compact form

$$J_2(t) \equiv \int^t \exp[J_1(t')]\left[G^{op} + \sum_{i=1}^{2} e_{ni}n_i(t') \right] dt'. \quad (26d)$$

This integral can be evaluated numerically. To add physical insight and evaluate the integral analytically without loss of precision, the adiabatic transport-rate time-gating assumption can be used consistently with regard to the earliest observation time, t_{min}, of any photothermal effect in the semiconductor with respect to the fast recombination time: $t_{min} \gg \tau_{1n}$, or

$$\frac{t_{\min}}{\tau_{1n}} \gg \sum_{i=1}^{2} A_{ni} \exp(-F_i t_{\min}) \quad \text{so that}$$

$$\int^t \exp\left(\frac{t'}{\tau_{1n}} - A_{ni} e^{-F_i t'}\right) dt' \simeq \int^t \exp\left(\frac{t'}{\tau_{1n}}\right) dt'. \tag{27}$$

This approximation has been tested with SI-GaAs and other direct-gap semiconductors and has been found to be satisfied for all times of relevance to thermal emission phenomena (>0.1 ms). Subject to this approximation the integrations in Eq. (26d) can be carried out to yield the expression

$$J_2(t) = \tau_{1n}\left\{ G^{\text{op}} + \sum_{j=1}^{2} e_{nj}(T) N_j P_j(T) \right.$$
$$\left. - \sum_{j=1}^{2} \left[\frac{e_{nj}(T) N_j \Delta P_j(T)}{1 - \tau_{1n} F_j}\right] e^{-F_j t} \right\} e^{t/\tau_{1n}}. \tag{28}$$

The initial conditions are defined in Eq. (15) for $t=0^-$, i.e., for times before the onset of illumination when the semiconductor is at thermal equilibrium. For electrons this condition becomes $n(0^-) = n_s(T)$, so that Eq. (26a) gives

$$K_1 = n_s(T) e^{J_1(0)} - J_2(0). \tag{29}$$

Finally, inserting Eq. (29) into Eq. (26a) gives the free-electron density during illumination as follows:

$$n(t,T) = \tau_{1n}\left\{ \left[G^{\text{op}} + \sum_{j=1}^{2} e_{nj}(T) N_j P_j(T) \right] (1 - e^{-t/\tau_{1n}}) \right.$$
$$- \sum_{j=1}^{2} \left[\frac{e_{nj}(T) N_j \Delta P_j(T)}{1 - \tau^{1n} F_j(T)} \right] (e^{-F_j t} - e^{-t/\tau_{1n}})$$
$$+ n_s(T) \exp\left[-\left(A_{n1} + A_{n2} \right.\right.$$
$$\left.\left.\left. + \frac{t}{\tau_{1n}} \right) \right] \right\} \exp\left(\sum_{i=1}^{2} A_{ni} e^{-F_i t} \right). \tag{30}$$

Equation (30) shows that the free-electron density quickly settles after an initial decay "spike" induced by the term $\exp(\sum_{i=1}^{2} A_{ni} e^{-F_i t})$. It then evolves with two kinds of time constants: $F_j^{-1}(T)$ and $\tau_{1n}(T)$. The former is photothermal (it includes both optical and thermal rate components); the latter is associated with a band-to-band recombination rate and a conduction band-to-trap or impurity state capture rate during the illumination phase. At times long compared to the effective recombination time constant τ_{1n} but consistent with thermal interactions between trap states and conduction band, the foregoing expression reduces to the superposition of the steady-state optical band-to-band excitation source and two electron sources originating in the emitting occupied trap states (N_1, E_1) and (N_2, E_2). These energy states build up the conduction band free-electron density with time constants F_j^{-1} as follows:

$$n(t,T) = \tau_{1n}\left(G^{\text{op}} + \sum_{j=1}^{2} e_{nj}(T) N_j P_j(T) \right.$$
$$\left. \times \left\{ 1 - \left[\frac{\Delta P_j(T)/P_j(T)}{1 - \tau_{1n} F_j(T)} \right] \exp(-F_j t) \right\} \right),$$
$$t \gg \tau_{1n}. \tag{31}$$

C. Hole-density kinetics during optical illumination: $0 \leq t \leq t_P$

The method used for deriving the free-electron density during illumination can be applied to the rate of free-hole density generation, Eq. (1d), with the trapped-carrier densities, Eq. (21), as inputs: In terms of time intervals, the optical recombination occurs much earlier ($\sim \tau_p$) than the thermal kinetics. Therefore, the steady nonequilibrium optical generation rate, G^{op}, can be separated out in the photothermal time evolution of the free-hole density. Rearranging Eq. (1d) in a manner similar to Eq. (23) for the free-electron density rate in the photothermal time range ($\gg \tau_{0p}$) yields

$$\frac{dp(t,T)}{dt} + \left\{ C_{p1} n_1(t,T) + C_{p2} n_2(t,T) + \frac{1}{\tau_p(T)} \right\} p(t,T)$$
$$= G^{\text{op}} + e_{p1}(T)[N_1 - n_1(t,T)] + e_{p2}(T)[N_2 - n_2(t,T)]. \tag{32}$$

The solution of this equation is

$$p(t) = K_2 \exp\left(-\int^t \left\{ \sum_{i=1}^{2} [C_{pi} n_i(t')] + \tau_p^{-1} \right\} dt' \right)$$
$$+ \exp\left(-\int^t \left\{ \sum_{i=1}^{2} [C_{pi} n_i(t')] + \tau_p^{-1} \right\} dt' \right)$$
$$\times \int^t \exp\left(\int^{t'} \left\{ \sum_{i=1}^{2} [C_{pi} n_i(y)] + \tau_p^{-1} \right\} dy \right)$$
$$\times \left\{ G^{\text{op}} + \sum_{i=1}^{2} e_{pi}[N_i - n_i(t')] \right\} dt'. \tag{33}$$

The constant K_2 is to be determined from the initial conditions immediately before the onset of the optical excitation as follows:

$$p(0^-) = p_s(T). \tag{34}$$

In a manner analogous to Eq. (26c), the following definition of the nonequilibrium capture to total photothermal emission-rate ratios for holes may be defined from Eqs. (17) and (22) as follows:

$$A_{pi}(T) \equiv C_{pi} N_i \left[\frac{\Delta P_i(T)}{F_i(T)} \right], \quad i = 1, 2. \tag{35}$$

A nonequilibrium photothermal relaxation lifetime of free holes into the two trap states can be defined in a form analogous to the thermal-equilibrium effective hole recombination time, Eq. (13),

$$\frac{1}{\tau_{1p}} \equiv \frac{1}{\tau_p} + \sum_{i=1}^{2} C_{pi} N_i P_i(T). \tag{36}$$

The solution (33) may be evaluated analytically within the framework of the adiabatic transport-rate time-gating assumption considering the earliest observation time of any photothermal effect involving hole kinetics in the semiconductor with respect to the fast hole recombination time: $t_{\min} \gg \tau_{1p}$, or

$$\frac{t_{\min}}{\tau_{1p}} \gg \sum_{i=1}^{2} A_{pi} \exp(-F_i t_{\min}) \quad \text{so that}$$

$$\int^t \exp\left(\frac{t'}{\tau_{1p}} - A_{pi} e^{-F_i t'}\right) dt' \simeq \int^t \exp\left(\frac{t'}{\tau_{1p}}\right) dt'. \tag{37}$$

Finally, the free-hole density in the valence band can be written as

$$p(t,T) = \tau_{1p} \left\{ \left(G^{\mathrm{op}} + \sum_{j=1}^{2} e_{pj}(T) N_j [1 - P_j(T)] \right) (1 - e^{-t/\tau_{1p}}) \right.$$
$$+ \sum_{j=1}^{2} \left[\frac{e_{pj}(T) N_j \Delta P_j(T)}{1 - \tau_{1p} F_j(T)} \right] (e^{-F_j t} - e^{-t/\tau_{1p}})$$
$$\left. + p_s(T) \exp\left(A_{p1} + A_{p2} - \frac{t}{\tau_{1p}} \right) \right\}$$
$$\times \exp\left(-\sum_{i=1}^{2} A_{pi} e^{-F_i t} \right). \tag{38}$$

At times long compared to the effective hole recombination time constant τ_{1p}, Eq. (38) reduces to the superposition of the steady-state optical band-to-band excitation source and two hole acceptor levels originating in the electron occupied fractions of the trap states (N_1, E_1) and (N_2, E_2). Through decay of trapped electrons to the valence band, these two energy states deplete the valence band free-hole density with the same time constants, F_j^{-1}, as the free-electron emission rates to the conduction band as follows:

$$p(t,T) = \tau_{1p} \left\{ G^{\mathrm{op}} + \sum_{j=1}^{2} e_{pj}(T) N_j [1 - P_j(T)] \right.$$
$$\left. \times \left[1 + \left(\frac{\Delta P_j(T)/[1 - P_j(T)]}{1 - \tau_{1p} F_j(T)} \right) \exp(-F_j t) \right] \right\},$$
$$t \gg \tau_{1p}. \tag{39}$$

D. Electron- and hole-density kinetics after optical pulse cutoff: $t \geq t_P$

Immediately after turning off the optical super-band-gap radiation source at $t = t_P$, the rate-gating principle can be applied to adiabatically isolate the photoexcited electron-density component of Eq. (7) as follows:

$$\frac{d\Delta n_{\mathrm{op}}(t)}{dt} = -\left\{ C_{n1}[N_1 - n_1(t)] + C_{n2}[N_2 - n_2(t)] \right.$$
$$\left. + \frac{1}{\tau_n} \right\} \Delta n_{\mathrm{op}}(t) \simeq -\left\{ C_{n1}[N_1 - n_1(t_P)] \right.$$
$$\left. + C_{n2}[N_2 - n_2(t_P)] + \frac{1}{\tau_n} \right\} \Delta n_{\mathrm{op}}(t), \quad t \geq t_P. \tag{40}$$

The adiabatic approximation of replacing the trapped-carrier density distribution at times $t > t_P$ with that attained at $t = t_P$ is valid for fast recombination lifetimes $\tau_n \ll F_j^{-1}(T)$; $j = 1, 2$, also assuming that ejection of trapped electrons occurs mainly thermally following the optical pulse cutoff. Introducing the following definition into Eq. (21):

$$n_j(t_P) \equiv n_{jP} = N_j \{ P_j(T) - \Delta P_j(T) \exp[-F_j(T) t_P] \}, \quad j = 1, 2, \tag{41}$$

Eq. (40) describes the decay of the optically excited electron population after pulse cutoff

$$\Delta n_{\mathrm{op}}(t > t_P) = \Delta n_{\mathrm{op}}(t_P) \exp\left[-\left(\frac{t - t_P}{\tau_{an}} \right) \right] \tag{42}$$

with a decay time constant (effective electron recombination lifetime), τ_{an}, shorter than the band-to-band recombination lifetime τ_n as follows:

$$\frac{1}{\tau_{an}} = \frac{1}{\tau_n} + \sum_{i=1}^{2} C_{ni}(N_i - n_{iP}). \tag{43}$$

τ_{an} involves additional capture rates into all empty trap states. Since the optical stimulus is turned off, the trapped-carrier density rate equations (1b) and (1c) involve only thermal rate components from Eqs. (3) and (6) as follows:

$$\frac{dn_1(t)}{dt} = -e_{n1}^{\mathrm{th}} n_1(t) + C_{n1} n_a(t)[N_1 - n_1(t)]$$
$$+ e_{p1}^{\mathrm{th}}[N_1 - n_1(t)] - C_{p1} p_a(t) n_1(t),$$

$$\frac{dn_2(t)}{dt} = -e_{n2}^{\mathrm{th}} n_2(t) + C_{n2} n_a(t)[N_2 - n_2(t)]$$
$$+ e_{p2}^{\mathrm{th}}[N_2 - n_2(t)] - C_{p2} p_a(t) n_2(t), \tag{44}$$

where

$$n_a(t,T) \equiv n_s(T) + \Delta n(t_P) \exp\left[-\left(\frac{t - t_P}{\tau_{an}} \right) \right],$$

$$p_a(t,T) \equiv p_s(T) + \Delta p(t_P) \exp\left[-\left(\frac{t - t_P}{\tau_{ap}} \right) \right]. \tag{45}$$

In a manner similar to Eq. (40) the adiabatic treatment of the free-hole density equation (1d) yields the effective hole recombination lifetime

$$\frac{1}{\tau_{ap}} = \frac{1}{\tau_p} + \sum_{i=1}^{2} C_{pi} n_{iP}. \tag{46}$$

Equation (45) shows that at long postoptical cutoff times $t - t_P \gg (\tau_{ap}, \tau_{an})$ on the order of the thermal emission time scales, the excess free-carrier densities decay to the respective thermal-equilibrium densities $n_a(t,T) \sim n_s(T)$ and $p_a(t,T) \sim p_s(T)$. Therefore, the trapped-carrier densities in states (E_1, N_1) and (E_2, N_2) can be found from Eq. (44) and initial conditions evaluated from Eq. (41) at an instant shortly after optical cutoff at $t = t_P^+$ when the total photothermal nonequilibrium transport rate, Eq. (17), changes abruptly to the thermal transport rate, Eq. (19), $F_j(T) \mapsto F_j^{\text{th}}(T)$. The results of the solution of the two initial-value problems for the time evolution of the trapped electron densities are

$$n_j(t,T) = P_j^{\text{th}}(T) N_j + [n_{jP}(T) - P_j^{\text{th}}(T) N_j]$$
$$\times \exp[-F_j^{\text{th}}(T)(t - t_P)], \quad j = 1, 2. \tag{47}$$

It is clear that the postoptical cutoff trapped-carrier populations are solely controlled by thermal probabilities and processes described by Eqs. (19) and (20) with the goal to return these populations to their equilibrium values. Once the time dependence of the trapped-carrier densities in the band-gap states is known, they can be used in Eqs. (1a) and (1d) with $G(t)^{\text{op}} = 0$ to calculate the free-carrier densities. For electrons Eq. (1a) becomes

$$\frac{dn(t,T)}{dt} + \left\{ C_{n1}[N_1 - n_1(t,T)] + C_{n2}[N_2 - n_2(t,T)] \right.$$
$$\left. + \frac{1}{\tau_n(T)} \right\} n(t,T) = e_{n1}^{\text{th}}(T) n_1(t,T) + e_{n2}^{\text{th}}(T) n_2(t,T). \tag{48}$$

The solution follows the method introduced in the context of Eq. (23) with the modified (thermal) simplification equivalent of Eq. (27) as follows:

$$\frac{t_{\min}}{\tau_{1n}^{\text{th}}} \gg \sum_{i=1}^{2} A_{ni}^{\text{th}}(1 - e^{-F_i t_P}) \exp[-F_i^{\text{th}}(t_{\min} - t_P)]. \tag{49}$$

In analogy to the photothermal decay time constant, Eq. (25), postoptical cutoff kinetics involves the thermal occupation probabilities $P_i^{\text{th}}(T)$ as follows:

$$\frac{1}{\tau_{1n}^{\text{th}}} \equiv \frac{1}{\tau_n} + \sum_{i=1}^{2} C_{ni} N_i [1 - P_i^{\text{th}}(T)] \tag{50}$$

as well as the nonequilibrium capture to total thermal transport-rate ratios for electrons, analogous to its photothermal counterpart $A_{ni}(T)$, Eq. (26c),

$$A_{ni}^{\text{th}}(T) \equiv C_{ni} N_i \left[\frac{\Delta P_i(T)}{F_i^{\text{th}}(T)} \right], \quad i = 1, 2. \tag{51}$$

Finally, the free-electron density is given by

$$n(t,T) = \left(\sum_{i=1}^{2} \tau_{1n}^{\text{th}} e_{ni}^{\text{th}} \left\{ P_i^{\text{th}}(T) N_i [1 - e^{-(t-t_P)/\tau_{1n}^{\text{th}}}] \right. \right.$$
$$\left. + \left[\frac{n_{ip} - N_i P_i^{\text{th}}(T)}{1 - \tau_{1n}^{\text{th}} F_i^{\text{th}}(T)} \right] [e^{-F_i^{\text{th}}(t-t_P)} - e^{-(t-t_P)/\tau_{1n}^{\text{th}}}] \right\}$$
$$\left. + n(t_p) \exp\left[\sum_{i=1}^{2} A_{ni}^{\text{th}}(1 - e^{-F_i t_P}) \right] e^{-(t-t_P)/\tau_{1n}^{\text{th}}} \right)$$
$$\times \exp\left[-\sum_{i=1}^{2} A_{ni}^{\text{th}}(1 - e^{-F_i t_P}) e^{-F_i^{\text{th}}(t-t_P)} \right], \tag{52}$$

where the carrier density $n(t_P)$ is given by Eq. (31) evaluated at the cutoff instant $t = t_P^-$.

In a manner similar to the onset of the free-electron density buildup during the illumination period which exhibits a sharp decay, Eq. (30), this equation predicts a sharp increase (spike) in the free-electron density immediately after optical turnoff induced by the term $\exp[-\sum_{i=1}^{2} A_{ni}^{\text{th}}(1 - e^{-F_i t_P}) e^{-F_i^{\text{th}}(t-t_P)}]$. For the usual experimental case of observation times $t \gg \tau_{1n}^{\text{th}}$, Eq. (52) simplifies to a free-electron density decay

$$n(t,T) \simeq \tau_{1n}^{\text{th}}(T) \sum_{j=1}^{2} e_{nj}^{\text{th}}(T) \left\{ N_j P_j^{\text{th}}(T) \right.$$
$$\left. + \left[\frac{n_{jP} - N_j P_j^{\text{th}}(T)}{1 - \tau_{1n}^{\text{th}}(T) F_j^{\text{th}}(T)} \right] \exp[-F_j^{\text{th}}(T)(t - t_P)] \right\}. \tag{53}$$

This is an excess thermal electron density decay. This expression is the result of the linear superposition of two independently decaying exponentials with time constants $(F_1^{\text{th}})^{-1}$ and $(F_2^{\text{th}})^{-1}$. As $t \mapsto \infty$, the excess electron density saturates at the value

$$n_{\text{eq}}(T) = n(t \to \infty) = \tau_{1n}^{\text{th}}(T) \sum_{j=1}^{2} e_{nj}^{\text{th}}(T) N_j P_j^{\text{th}}(T). \tag{54}$$

It is straightforward to prove that this value is identical to the one obtained from the rate equation (1a) at the steady state, $dn(t,T)/dt = 0$, with $G^{\text{op}} = 0$, $e_{nj}(T) = e_{nj}^{\text{th}}(T)$, and equilibrium trapped-carrier densities $n_j(\infty, T) = P_j^{\text{th}}(T) N_j$, $j = 1, 2$, from Eq. (47). The resulting equation is

$$n_{\text{eq}}(T) = n(t \to \infty)$$
$$= \frac{e_{n1}^{\text{th}}(T) N_1 P_1^{\text{th}}(T) + e_{n2}^{\text{th}}(T) N_2 P_2^{\text{th}}(T)}{C_{n1} N_1 [1 - P_1^{\text{th}}(T)] + C_{n2} N_2 [1 - P_2^{\text{th}}(T)] + \tau_n^{-1}}, \tag{55}$$

which is the same as Eq. (54) when the definition of $\tau_{1n}^{\text{th}}(T)$, Eq. (25), is taken into account.

Following optical pulse cutoff, the free-hole density can be calculated using the same procedure as that for free electrons: First, the expressions for the trapped-carrier densities $n_1(t)$ and $n_2(t)$ are inserted in Eq. (1d) and the inhomogeneous initial-value problem with an initial condition at $t = t_P$ is defined. The solution is

$$p(t,T) = \left(\sum_{i=1}^{2} \tau_{1p}^{th} N_i e_{pi}^{th} \left\{ [1 - P_i^{th}(T)][1 - e^{-(t-t_p)/\tau_{1p}^{th}}] \right.\right.$$
$$\left. - \left[\frac{\Delta P_i^{th}(T)(1 - e^{-F_i t_P})}{1 - \tau_{1p}^{th} F_i^{th}(T)} \right] [e^{-F_i^{th}(t-t_P)} - e^{-(t-t_p)/\tau_{1p}^{th}}] \right\}$$
$$+ p(t_p) \exp\left[-\sum_{i=1}^{2} A_{pi}^{th}(1 - e^{-F_i t_P}) \right] e^{-(t-t_p)/\tau_{1p}^{th}} \right)$$
$$\times \exp\left[\sum_{i=1}^{2} A_{pi}^{th}(1 - e^{-F_i t_P}) e^{-F_i^{th}(t-t_p)} \right], \tag{56}$$

where, in analogy to Eq. (50), the total thermal decay time constant for holes

$$\frac{1}{\tau_{1p}^{th}(T)} \equiv \frac{1}{\tau_p} + \sum_{i=1}^{2} C_{pi} N_i P_i^{th}(T) \tag{57}$$

was used, along with the nonequilibrium capture to total thermal transport-rate ratio for holes in band-gap state (i), the counterpart of $A_{ni}^{th}(T)$, Eq. (51),

$$A_{pi}^{th}(T) \equiv C_{pi} N_i \left[\frac{\Delta P_i(T)}{F_i^{th}(T)} \right], \quad i = 1, 2. \tag{58}$$

In Eq. (56) the value of the free-hole density at the optical cutoff instant, $p(t_P)$, can be determined from Eq. (39) evaluated at $t = t_P$. For experimental observation times $t \gg \tau_{1p}^{th}$, Eq. (56) simplifies to a free-hole density increase

$$p(t,T) \simeq \tau_{1p}^{th}(T) \sum_{j=1}^{2} e_{pj}^{th}(T) N_j \left\{ 1 - P_j^{th}(T) \right.$$
$$\left. - \left[\frac{\Delta P_j(T)(1 - e^{-F_j t_P})}{1 - \tau_{1p}^{th}(T) F_j^{th}(T)} \right] \exp[-F_j^{th}(T)(t - t_P)] \right\}. \tag{59}$$

This equation shows that the free-hole population following optical cutoff builds up to the thermal-equilibrium level

$$p_{eq}(T) = p(t \mapsto \infty, T) = \tau_{1p}^{th}(T) \sum_{j=1}^{2} e_{pj}^{th}(T) N_j [1 - P_j^{th}(T)] \tag{60}$$

as electrons from the valence band transition to the unoccupied trap states to restore equilibrium, following the depletion of those states via emissions to the conduction band as described by Eq. (53). It is straightforward to prove that Eq. (60) is identical to the one obtained from the rate equation (1d) for $t \to \infty$, at the steady state by proceeding as with the equilibrium electron-density equation (54) with $G^{op} = 0$, $e_{pj}(T) = e_{pj}^{th}(T)$, $n_j(\infty, T) = P_j^{th}(T) N_j$, $j = 1, 2$, from Eq. (47). The resulting equation yields

$$p_{eq}(T) = p(t \to \infty)$$
$$= \frac{e_{p1}^{th}(T) N_1 [1 - P_1^{th}(T)] + e_{p2}^{th}(T) N_2 [1 - P_2^{th}(T)]}{C_{p1} N_1 P_1^{th}(T) + C_{n2} N_2 P_2^{th}(T) + \tau_p^{-1}}. \tag{61}$$

This is the same as Eq. (60) when the definition of $\tau_{1p}^{th}(T)$, Eq. (57), is taken into account.

III. DLPTS SIGNAL GENERATION THEORY

When a sub-band-gap laser impinges on a semiconductor with a nonequilibrium photoexcited free-carrier density, two kinds of absorption occur: one is free-carrier absorption (fca), and the other is deep level (defect) absorption (dla). Depending on the wavelength of the probe laser, fca is controlled by various mechanisms. In the near-infrared region, fca is mainly associated with intraband absorption, which is caused by excitation of electrons to a higher conduction band minimum. However, in the mid-infrared region, fca is mainly due to electron-phonon interactions.[22] Usually, the absorption coefficient α_{fca} is larger at longer wavelengths.[22] In the relaxation-time approximation in semiconductors, the energy-dependent relaxation time tensor, $\tau_{\mathbf{S}}$, has the same principal axes as the effective-mass tensor, $\mathbf{m}^*$, with principal values $\tau_{\parallel}$ and $\tau_{\perp}$, where the subscripts indicate directions parallel and perpendicular to the ellipsoidal constant energy surfaces. In the semiclassical theory of free-carrier contribution to the dielectric function of semiconductors, the Drude–Zener approximation is obtained for isotropic relaxation time, when the carrier density is degenerate. In that limit $\tau_{\mathbf{S}}$ reduces to a scalar, τ_S.[23] The result is the Drude equation for free-electron absorption coefficient α_{fca} with hole density $p \ll n$ as follows:

$$\alpha_{fca}(N) = \frac{n q^2 \lambda^2}{8 \pi^2 N c^3 m^* \tau_S} = \frac{n q^3 \lambda^2}{4 \pi^2 \varepsilon_0 N c^3 m^* \mu}, \tag{62}$$

where n is the free-electron density, m^* is the isotropic electron effective mass, N is the refractive index, c is the speed of light in the semiconductor, and μ is the carrier mobility. A similar expression is valid for p-type semiconductors, provided n is replaced by p, the free hole density. At a given sub-band-gap wavelength, α_{fca} is proportional to the free-carrier density, which can be expressed by $\alpha_{fca} = \sigma_{fca} n(t) \times [cm^{-1}]$, where σ_{fca} is the absorption cross section, considered constant within a wide temperature range of $\Delta T \sim 150$ K, such as the one used in our experiments.

dla absorption is caused by injection of carriers from a trap state (usually a deep level) to the conduction band. Strictly speaking, this type of absorption can only be observed when the photon energy is larger than the deep level activation energy. However, thermal effects can broaden the absorption cross section, σ_{dla}, significantly. This absorption has been commonly applied in the mapping of deep levels in semiconductors, for instance, the EL2 level in SI-GaAs.[24] The dla absorption coefficient can be written as $\alpha_{dla} = \sigma_{dla} n_T$, where n_T is the density of occupied states, and σ_{dla} could also be considered a constant in a temperature range of $\Delta T \sim 150$ K.
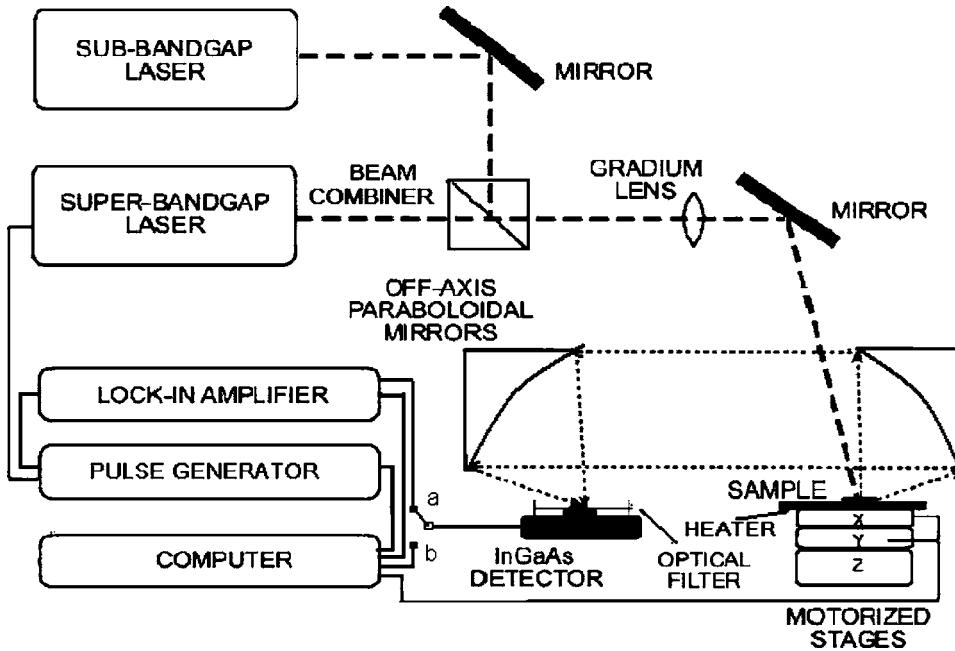
FIG. 2. Schematic diagram for DLPTS: (a) temperature-scanned approach and (b) time-scanned approach.

The measurement of absorption can be performed by either transmission or scattered (diffuse) reflection, where transmission is used in two-side-polished semiconductor crystals, while diffuse reflection is suitable for one-side-polished semiconductors with a natural matte back surface. Considering multiple internal reflections, the transmission signal from a two-side-polished sample of thickness d is given by[25]

$$T(t) = I_0 \frac{(1-R)^2 \exp(-\alpha d)}{1 - R^2 \exp(-2\alpha d)}, \qquad (63)$$

where R is the reflection coefficient. In the case of diffuse reflection, the backscattered signal can be written as

$$I(t) = I_0 \frac{(1-R)^2 S \exp(-2\alpha d)}{1 - RS \exp(-2\alpha d)}, \qquad (64)$$

where S represents the scattered reflection coefficient from the back surface.

Since the excitation laser beam penetrates only a few micrometers below the surface, the absorption coefficient corresponding to the probe wavelength is different on the surface and in the bulk of the wafer. αd in Eqs. (63) and (64) can be written as $\alpha d = \alpha_1 d_1 + \alpha_2 d_2$, where subscript 1 stands for the surface and subscript 2 represents the bulk. Since the sub-band-gap absorption coefficient is very low ($\alpha d \ll 1$) in high-resistivity materials and the bulk absorptance $\alpha_2 d_2$ is a constantly independent of the intensity and temporal shape of the laser pulse, Eqs. (63) and (64) may thus be simplified to

$$T(t) \approx I_0 \frac{(1-R)^2(1-\alpha_1 d_1)(1-\alpha_2 d_2)}{1-R^2} = L[1 - \alpha_1(t)d_1],$$
$$(65)$$

$$I(t) \approx I_0 \frac{(1-R)^2 S(1-2\alpha_1 d_1)(1-2\alpha_2 d_2)}{1 - RS}$$
$$= K[1 - 2\alpha_1(t)d_1], \qquad (66)$$

where $L \equiv I_0[(1-R)^2(1-\alpha_2 d_2)/(1-R^2)]$ and $K \equiv I_0[(1-R)^2 S(1-2\alpha_2 d_2)/(1-RS)]$ are constants independent of the intensity and temporal shape of the excitation pulse. In both cases, the signal depends linearly on α_1. The following discussion will be based on the backscattered signal, $I(t)$, which represents the only experimental mode used in this work.

Considering the absorption mechanisms discussed above, the backscattered signal $I(t)$ can be written as

$$I(t) = K[1 - 2\sigma_{\text{fca}}n(t)d_1 - 2\sigma_{\text{dla}}n_T(t)d_1]. \qquad (67)$$

The DLPTS signal is then a linear superposition of quantities proportional to the free-carrier concentration $n(t)$ and the density of the occupied states $n_T(t)$. If more than one discrete state are present in the semiconductor, the signal can be expressed as a superposition of contributions from all defect and trap states as follows:

$$I(t) = K\left[1 - 2d_1\sigma_{\text{fca}}n(t) - 2d_1\sum_{i=1}^{m}\sigma_{\text{dla}}^i n_{Ti}(t)\right], \qquad (68)$$

where m is the number of participating energy states. This possibility requires a straightforward extension of the theory in Sec. II from 2 to m energy levels in the band gap.

IV. EXPERIMENTAL CONFIGURATIONS

The schematic diagram of DLPTS is shown in Fig. 2. The sample is placed on a temperature controlled heating plate, which allows maintaining constant temperature in the $25-250$ °C range, or can provide temperature ramping. The excitation source is a periodic time-gated super-band-gap laser pulse ($\lambda = 830$ nm) emitting 20 mW (peak power) with a beam diameter in about 0.1 mm. The pulse parameters are controlled by a pulse generator, with the pulse width fixed at
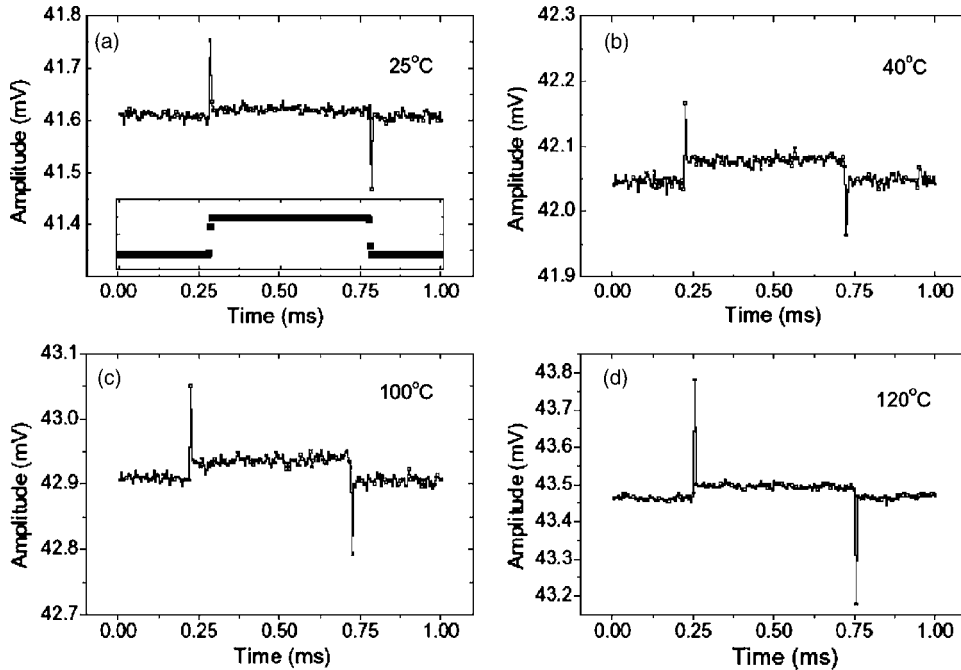
FIG. 3. PCR transients from a SI-GaAs wafer at 1 kHz repetition rate and at various temperatures. Inset in (a): optical waveform from excitation laser.

1% of the repetition period. Due to the high absorption coefficient of the super-band-gap beam ($\alpha \sim 10^4$ cm^{-1}), the pump laser penetrates only a few micrometers into the sample. The probe beam is from a coincident sub-band-gap dc laser ($\lambda = 1550$ nm) emitting 3 mW with approximately 0.15 mm diameter spot size. Samples used in this work are one-side-polished vertical gradient freeze (VGF) grown SI-GaAs wafers with a resistivity of $(7.2-7.7) \times 10^7$ Ω cm, etch pit density (EPD) <4000 cm^{-2}, and a EL2 concentration around 10^{16} cm^{-3} as provided by the vendor. The probe laser penetrates the entire thickness of the SI-GaAs wafer and is partly scattered by the naturally rough back surface of the sample. The scattered light is collected by two collimating off-axis paraboloidal mirrors and focused onto an InGaAs photodetector with a 1550 nm notch filter. For temperature-scanned DLPTS (switch a), the signal is fed into an AME-TEK 5210 lock-in amplifier, which functions as a rate window, while for time-scanned DLPTS (switch b), the raw signal is collected through a National Instruments PCI-6281 data acquisition (DAQ) card installed in the computer. The results are displayed simultaneously in the computer as a function of temperature and time, respectively.

V. EXPERIMENTAL RESULTS AND DISCUSSION

A. Time-scanned DLPTS transients

The theoretical predictions of Eqs. (30) and (52) for the free-electron density at the onset and cutoff of an optical pulse of duration t_P, respectively, as generalized to m band-gap trap states are (a) that at optical turnon a positive narrow free-carrier spike (assuming electrons are the dominant photoexcited carriers) will be induced and will decay quickly as described by the term $\exp(\Sigma_{i=1}^{m} A_{ni} e^{-F_i t})$ to the level predicted by the much more slowly evolving transient in the body of Eq. (30); after pulse cutoff at $t=t_P$, a negative narrow spike will appear and will fast build up as per $\exp[-\Sigma_{i=1}^{m} A_{ni}^{th}(1 - e^{-F_i t_P}) e^{-F_i^{th}(t-t_P)}]$ to the level of the much more slowly

changing transient in the body of Eq. (52). DLPTS, however, is a technique which involves both trapped absorption and fca, which may obscure the individual contributions. Therefore, we used time-domain photocarrier radiometry[26] (PCR) to test these purely free-carrier predictions of IR-photon emissions due to radiative band-to-band recombination in SI-GaAs. The PCR signal depends on the density of the photogenerated excess diffusive carrier density, $n(t)$. In one dimension it can be expressed by the equation[26]

$$S_{1-D}(t) \approx H(\lambda_1, \lambda_2) \int_0^L \alpha_{\text{fca}}[n(z, t; \lambda)] dz, \qquad (69)$$

where H is a function of the surface reflectivity of the semiconductor, its radiative quantum efficiency, and the spectral power per unit wavelength (the product of recombination transition rate from band to band, or from bandedge to defect or impurity state, as the case may be, and the energy difference between initial and final states). L is the thickness of the semiconductor and λ_1 and λ_2 are the limits of the spectral bandwidth of the IR detector, $\lambda_1 \leqslant \lambda \leqslant \lambda_2$. Figure 3 shows this type of optical switch-on/switch-off phenomena in SI-GaAs at several temperatures with optical pulse repetition rate set at 1 kHz. It can be clearly seen that the turn-on spike is positive, decreasing to the illumination steady-state value and the turn-off spike is negative, increasing to the dark steady-state value.

Figure 4 shows the DLPTS time-scanned transient at various temperatures. All of the transients consist of three parts: (a) a sharp decrease of the signal at the beginning of the pulse, followed by (b) a rapid increase of the signal at the end of the pulse, also followed by (c) a slower long-time recovery of the signal. The rapid decrease is caused by the generation of free carriers by the excitation pulse which increase the IR absorption coefficient and thus decrease the DLPTS signal in diffuse reflection after a round-trip across the bulk of the semiconductor, while the fast increase is due
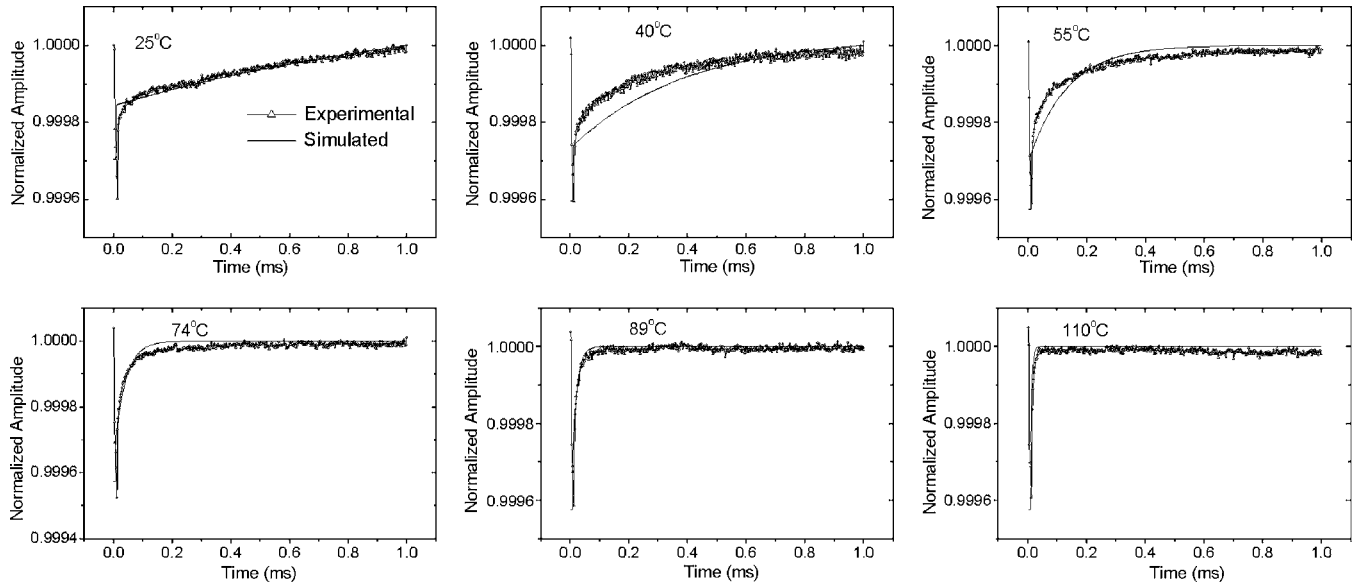
FIG. 4. The experimental and best-fitted (simplified single-level theory) DLPTS transients at various temperatures.

to the recombination of free carriers and restoration of the near-IR transparency of the material. This part is similar in temporal behavior to the PCR signals of Fig. 3, but for viewing in a transmission, rather than absorption, mode. The slow recovery is a result of thermal emission of carriers from deep level states in the band gap. Assuming a distribution of discrete energy states m, the physical process can be described by the following equations using the multitrap transport-rate time-gating theory. The theory is relevant to SI-GaAs carrier kinetics as the band-to-band recombination time is extremely short ($\sim$ns) compared to thermal emission times ($\geqslant 100$ μs). Equations (30) and (52) when generalized to m levels with trap densities $N_{T1}, N_{T2}, \ldots, N_{Tm}$ can be rewritten as

$$n(t,T) = \tau_{1n}\left\{\left[G^{\mathrm{op}} + \sum_{i=1}^{m} e_{ni}N_{Ti}P_i(T)\right](1 - e^{-t/\tau_{1n}}) - \sum_{i=1}^{m}\left[\frac{e_{ni}N_{Ti}\Delta P_i(T)}{1 - \tau_{1n}F_i(T)}\right](e^{-F_it} - e^{-t/\tau_{1n}})\right.$$

$$\left. + \frac{n_s(T)}{\tau_{1n}}e^{-(A_{n1}+A_{n2}+t/\tau_{1n})}\right\}\exp\left[\sum_{i=1}^{m}A_{ni}e^{-F_it}\right], \quad t \leqslant t_P \tag{70}$$

and

$$n(t,T) = \left(\sum_{i=1}^{m}\tau_{1n}^{\mathrm{th}}e_{ni}^{\mathrm{th}}\left\{P_i^{\mathrm{th}}(T)N_{Ti}[1 - e^{-(t-t_p)/\tau_{1n}^{\mathrm{th}}}] + \left[\frac{n_{Tip} - N_{Ti}P_i^{\mathrm{th}}(T)}{1 - \tau_{1n}^{\mathrm{th}}F_i^{\mathrm{th}}(T)}\right][e^{-F_i^{\mathrm{th}}(t-t_p)} - e^{-(t-t_p)/\tau_{1n}^{\mathrm{th}}}]\right\}\right.$$

$$\left. + n(t_p)\exp\left[\sum_{i=1}^{m}A_{ni}^{\mathrm{th}}(1 - e^{-F_it_p})\right]e^{-(t-t_p)/\tau_{1n}^{\mathrm{th}}}\right)\exp\left[-\sum_{i=1}^{m}A_{ni}^{\mathrm{th}}(1 - e^{-F_it_p})e^{-F_i^{\mathrm{th}}(t-t_p)}\right], \quad t \leqslant t_P \tag{71}$$

For energy state i, C_{ni} is the capture coefficient, $n_{Ti}(t_P)$ is the density of occupied states at the end of the filling pulse, and $e_{ni}(T)$ is the thermal emission rate given from Eq. (2) by $e_{ni}(T) = \gamma_{ni}\sigma_i T^2 \exp(-E_{ni}/kT)$, where γ_{ni} is equal to 2.67 $\times 10^{20}$ cm^{-2} s^{-1} K^{-2} for GaAs. σ_i is the electronic capture cross section by the deep level; in addition, $\tau_{1n} \equiv 1/\{1/\tau_n + \sum_{i=1}^{m}C_{ni}N_{iT}[1 - P_i(T)]\}$, $\tau_{1n}^{\mathrm{th}} \equiv 1/\{1/\tau_n + \sum_{i=1}^{m}C_{ni}N_{iT}[1 - P_i^{\mathrm{th}}(T)]\}$ are the generalized effective free-carrier lifetimes during and after the pulse, given by Eqs. (25) and (50), respectively, when $m=2$. $A_{ni} \equiv C_{ni}N_{Ti}[\Delta P_i(T)/F_i(T)]$, $A_{ni}^{\mathrm{th}} \equiv C_{ni}N_{Ti}[\Delta P_i(T)/F_i^{\mathrm{th}}(T)]$ represent the nonequilibrium capture processes during and after the optical pulse, Eqs. (26c) and (51), respectively.

The DLPTS signal then can be expressed as follows:

$$I(t) = K\left\{1 - 2\sigma_{\text{fca}}d_1\left(\tau_{1n}\left\{\left[G^{\text{op}} + \sum_{i=1}^{m} e_{ni}N_{Ti}P_i(T)\right](1 - e^{-t/\tau_{1n}}) - \sum_{i=1}^{m}\left[\frac{e_{ni}N_{Ti}\Delta P_i(T)}{1 - \tau_{1n}F_i(T)}\right](e^{-F_i t} - e^{-t/\tau_{1n}})\right.\right.\right.$$

$$\left.\left.\left. + \frac{n_s(T)}{\tau_{1n}}e^{-(A_{n1}+A_{n2}+t/\tau_{1n})}\right\}\exp\left[\sum_{i=1}^{m}A_{ni}e^{-F_i t}\right]\right) - 2d_1\sum_{i=1}^{m}\sigma_{dla}^i N_{Ti}[P_i(T) - \Delta P_i(T)e^{-F_{1i}t}]\right\}, \quad (72)$$

and

$$I(t) = K\left\{1 - 2\sigma_{\text{fca}}d_1\left[\left(\sum_{i=1}^{m}\tau_{1n}^{\text{th}}e_{ni}^{\text{th}}\left\{P_i^{\text{th}}(T)N_{Ti}[1 - e^{-(t-t_p)/\tau_{1n}^{\text{th}}}] + \left[\frac{n_{Tip} - N_{Ti}P_i^{\text{th}}(T)}{1 - \tau_{1n}^{\text{th}}F_i^{\text{th}}(T)}\right][e^{-F_i^{\text{th}}(t-t_p)} - e^{-(t-t_p)/\tau_{1n}^{\text{th}}}]\right\}\right.\right.\right.$$

$$\left.\left.\left. + n(t_p)\exp\left[\sum_{i=1}^{m}A_{ni}^{\text{th}}(1 - e^{-F_i t_p})\right]e^{-(t-t_p)/\tau_{1n}^{\text{th}}}\right)\exp\left[-\sum_{i=1}^{m}A_{ni}^{\text{th}}(1 - e^{-F_i t_p})e^{-F_i^{\text{th}}(t-t_p)}\right]\right] - 2d_1\sum_{i=1}^{m}\sigma_{dla}^i n_{Ti}(t)\right\} \quad t \geq t_p \quad (73)$$

By neglecting the hole-emission and capture processes, the temperature-dependent background free-carrier density, and the trap occupation probabilities under dark (thermal) conditions ($P_j^{\text{th}} \ll P_j$); and by assuming an ultrafast recombination lifetime τ_n compared to the earliest observation time, the complete multiple m-level theory yields simplified expressions in lieu of Eqs. (70) and (71) as follows: For $t \leq t_P$

$$n(t,T) = G^{\text{op}}\tau_n\left\{1 + \sum_{j=1}^{m}N_j C_{nj}\tau_n[1 - e^{-(e_{nj}+C_{nj}G^{\text{op}}\tau_n)t}]\right\} \quad (74)$$

for the free-carrier density; and

$$n_T(t,T) \equiv \sum_{i=0}^{m}n_{Ti}(t,T)$$

$$= \sum_{i=0}^{m}\frac{N_{Ti}}{1 + (e_{ni}/G^{\text{op}}\tau_n C_{ni})}[1 - e^{-(G^{\text{op}}\tau C_{ni}+e_{ni})t}]. \quad (75)$$

The respective expressions for $t \geq t_P$ are

$$n(t,T) = \tau_n\sum_{j=1}^{m}e_{nj}^{\text{th}}(T)N_j\left[\frac{1 - e^{-(e_{nj}+C_{nj}G^{\text{op}}\tau_n)t_P}}{1 + (e_{nj}/C_{nj}G^{\text{op}}\tau_n)}\right]$$

$$\times\exp[-e_{nj}^{\text{th}}(t-t_P)] \quad (76)$$

and

$$n_T(t,T) = \sum_{j=1}^{m}N_j\left[\frac{1 - e^{-(e_{nj}+C_{nj}G^{\text{op}}\tau_n)t_P}}{1 + (e_{nj}/C_{nj}G^{\text{op}}\tau_n)}\right]\exp[-e_{nj}^{\text{th}}(t-t_P)]. \quad (77)$$

In the special case of a single participating energy level (i), Eqs. (74)–(76) can be simplified to the simple one-level theory which has been commonly used in DLTS and PITS measurements.[27] For $t \leq t_p$

$$n(t) = G^{\text{op}}\tau(1 - e^{-t/\tau}) \quad (78)$$

and

$$n_{Ti}(t) = \frac{N_T}{1 + (e_{ni}/G^{\text{op}}\tau C_n)}[1 - e^{-(G^{\text{op}}\tau C_n+e_n)t}]. \quad (79)$$

For $t \geq t_p$

$$n(t) = M[e^{-(t-t_P)e_n} - e^{-(t-t_P)/\tau}] + n(t_P)e^{-(t-t_P)/\tau}, \quad (80)$$

$$M \equiv n_T(t_P)\left(\frac{e_n}{\tau^{-1} - e_n}\right)$$

and

$$n_T(t) = n_T(t_P)e^{-e_n(t-t_P)}. \quad (81)$$

Using parameters associated with the EL3 level in SI-GaAs, the DLPTS transient was simulated with the simplified one-state theory in Eqs. (68) and (78)–(81). The simulation results are shown in Fig. 4, while the parameters giving the best fits are listed in Table I. The other parameters used in the simulation, including material constants, are given in Table II. The best-fitted transients clearly exhibit the expected three parts of the signal; however, the recovery curves do not fit the experimental data very well, especially at low temperatures. Considering that high temperature transients may consist of fewer participating states owing to the thermal depletion of shallower levels, the discrepancies at low temperatures are assumed to be the result of multiple energy-state participation to the time-resolved signal. To verify this, two more discrete energy states were added to the transient

TABLE I. The values of band-gap energy-state parameters extracted from the best fit to the data involving a single trap-state energy.

	E_n (eV)	σ_n (cm^2)	σ_{dla} (cm^2)	N_T (cm^{-3})
EL3 Level	0.58	2.7×10^{-13}	3×10^{-18}	0.5×10^{-16}

TABLE II. Parameters used in the simulation.

	σ_{fca} (cm^2)	g_{op} (cm^{-3} s^{-1})	τ (s)	γ_n (cm^{-2} s^{-1} K^{-2})
SI-GaAs	3×10^{-18}	1×10^{-24}	1×10^{-8}	2.67×10^{20}
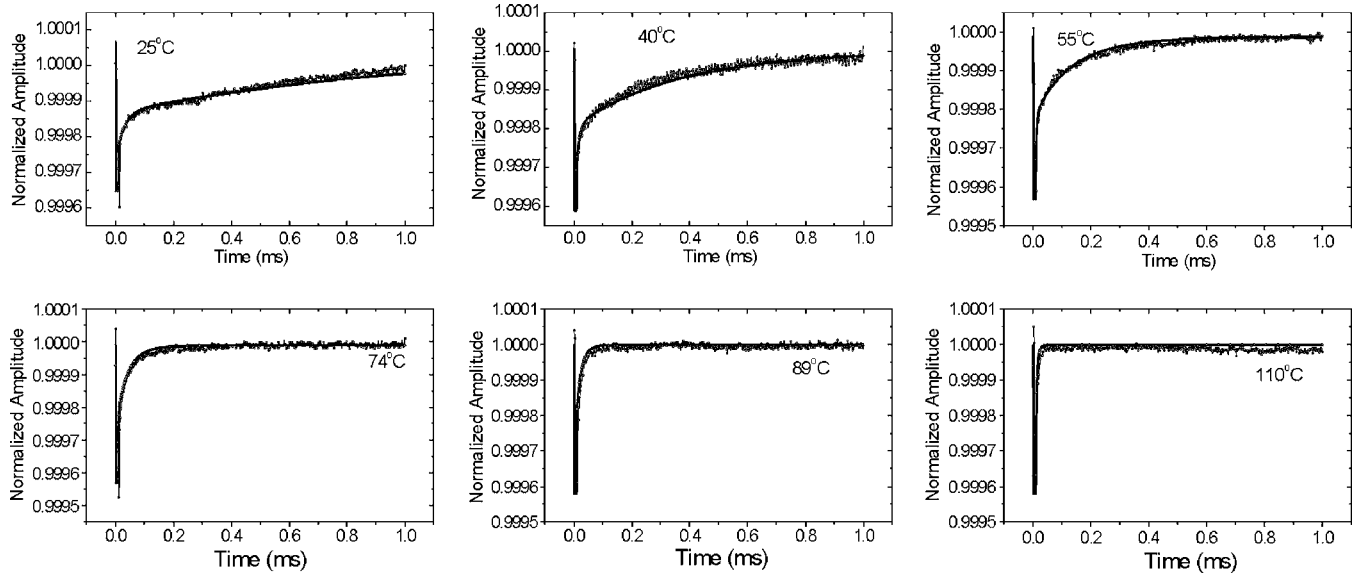
FIG. 5. The experimental and best-fitted (simplified three-level theory) DLPTS transients. Superposed are best-fit theoretical curves using the complete three-level theory.

using Eqs. (78)–(81). Figure 5 shows the results and Table III gives the best-fit values of the activation energies. The values for σ_n used were obtained from Table I, and the values for σ_{dla} were assumed to be the same as the σ_{fca}.[22] For the values of N_T, they were assumed to be on the order of the EL2 level concentration as measured independently. The other parameters used in the simulation are the same as in Table II. Based on the literature,[4,27] the three levels were identified as EL4, EL3, and HL3. All these levels have been commonly observed in VGF grown GaAs samples, and their physical origins have been discussed in Ref. 4. The most well-known EL2 level in SI-GaAs is not detectable in this measurement; this is due to the small dla absorption coefficient of EL2 level at the 1550 nm (0.8 eV) probe wavelength.[24] In order to detect the EL2 level, a shorter wavelength probe, usually around 1 μm, must be used. A DLPTS system with 980 nm probe light is now under development in our laboratory.

It should be noticed that the number of defect/impurity levels that can be identified with DPTLS depends on the temperature and time ranges of the experiment. Shallow levels have very fast emission rates above room temperature hence they cannot be identified within the temperature and time ranges of these transients. The existence of these three levels in above-room-temperature transients has also been confirmed in our inverse Laplace calculations, which reveal three discrete peaks in the inverse spectrum.[28] Compared with the single-state theory, the three-state model gives a much better fit to the experimental result at all temperatures.

Small discrepancies mainly at the beginning of the laser pulse may be due either to the influence of the superposition of the previous pulse, which has not been taken into account in the theory, or to contributions from other shallower energy states which reach thermodynamic equilibrium at earlier times through faster transients than the experimental time range of these measurements.

Using the parameters in Table II, another simulation was performed based on the complete three-state theory equations (72) and (73). The best fits were basically the same as those in the simplified three-state model. For ease of comparison, the two best-fitted transients are plotted together in Fig. 6. Differences appear mainly during times immediately after laser pulse turnon [Fig. 6(b)], while transients after the pulse are essentially identical. Since SI-GaAs has an extrashort free-carrier recombination lifetime, this implies that the simplified multistate theory is valid for short lifetime semiconductors, in which hole-emission and capture processes can be neglected and thermal-equilibrium carrier populations are negligible compared to photoexcited free-carrier densities.

B. Temperature-scanned DLPTS spectrum

In temperature-scanned DLPTS, the original transient $I(t)$ is fed into the lock-in amplifier (LIA), which functions as a rate window, Fig. 2. In terms of in-phase and quadrature components, the LIA signal can be written, respectively, as[29]

$$X = \frac{1}{T_0}\int_0^{T_0} I(t)\sin(2\pi t/T_0)dt \tag{82}$$

and

$$Y = \frac{1}{T_0}\int_0^{T_0} I(t)\cos(2\pi t/T_0)dt, \tag{83}$$

or, in terms of amplitude and phase,

TABLE III. The values of band-gap energy-state parameters extracted from the best fits to the data involving three energy states.

	E_n (eV)	σ_n (cm^2)	σ_{dla} (cm^2)	N_T (cm^{-3})
Level 1 (EL4)	0.49	2.7×10^{-13}	3×10^{-18}	0.5×10^{-16}
Level 2 (EL3)	0.58	2.7×10^{-13}	3×10^{-18}	0.5×10^{-16}
Level 3 (HL3)	0.60	2.7×10^{-13}	3×10^{-18}	0.5×10^{-16}
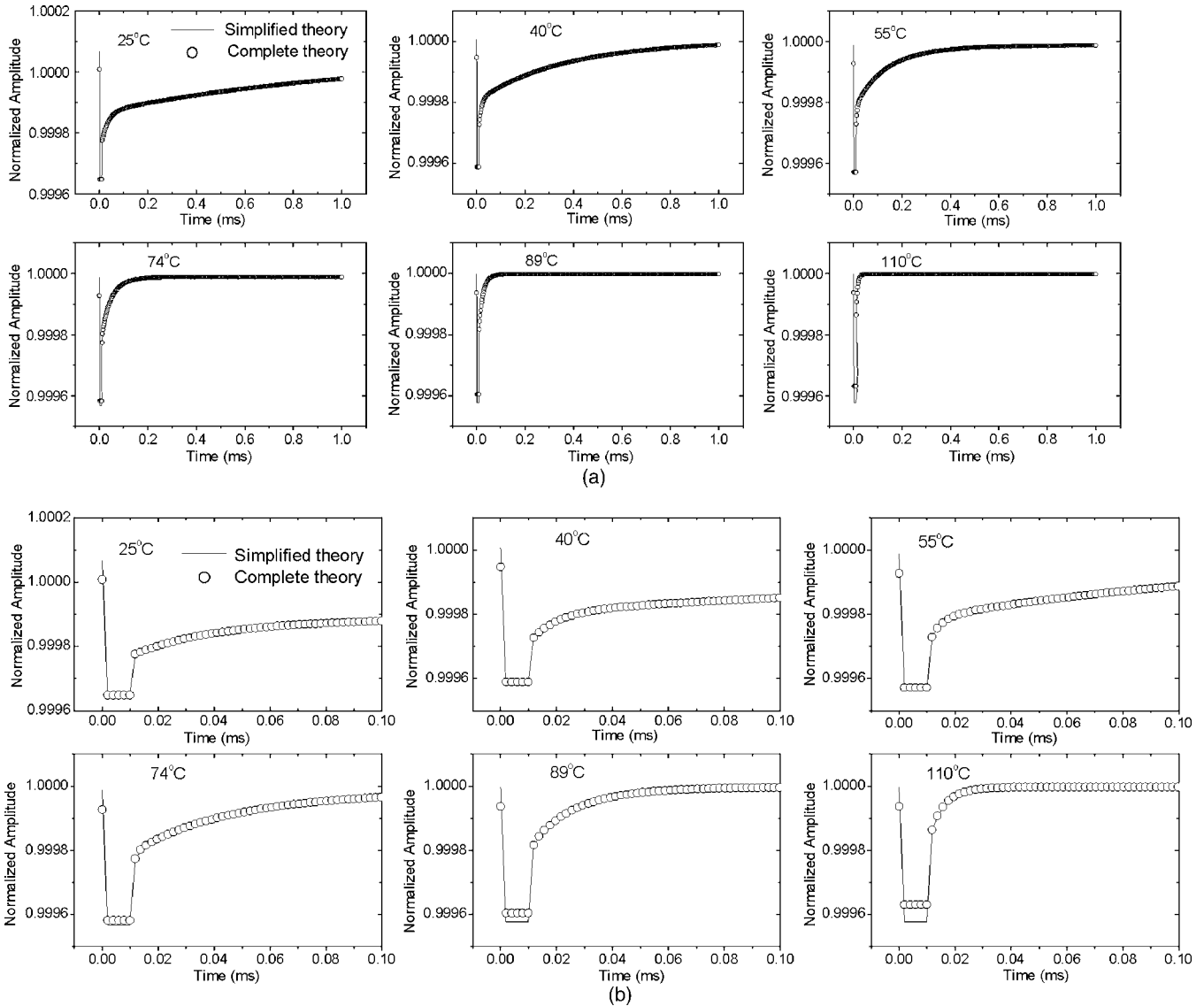
FIG. 6. Comparison of best-fitted theoretical transients based on the simplified (lines) and complete (circles) three-level theory ($m=3$). (a) Full-range transients; (b) early-time transients.

$$R = \sqrt{X^2 + Y^2} \tag{84}$$

and

$$\theta = \tan^{-1}(Y/X). \tag{85}$$

Here $T_0 = 1/f$, is the pulse repetition period and $I(t)$ is given in Eq. (68).

Figure 7(a) shows the temperature-scanned DLPTS spectrum of SI-GaAs at 1 kHz with the theoretical spectra calculated based on Eqs. (68)–(81), (84), and (85), and parameters in Tables I (single level) and II (three levels). A peak, which is characteristic of the dominant energy level, is observed in the amplitude channel of the spectrum. In agreement with the time-scanned transients, three-level simulations from both simplified and complete theories give better fits than the single-level theory. It was found that the complete three-level theory gave the best fit among all three curves in both amplitude and phase channels. To clarify the

effect of the EL4 level, Fig. 7(b) gives a comparison of the superposition of two-level (EL3, HL3) and three-level (EL3, EL4, HL3) spectra. Consistently with our time-domain transient, the EL4 level results in a slight shift toward the experimental curve in both the amplitude and phase channel at the low temperature end, and it also introduces some broadening to the peak of the amplitude channel. For better understanding of the trap-state superposition effects on the lineshape of the photothermal spectra from three levels, Fig. 8 shows temperature-resolved component spectra from each contributing energy level. The figure reveals that the peak in the amplitude channel is actually the result of the superposition of two peaks contributed from the EL3 and HL3 energy levels. The linewidth is affected by all three energy levels, although the peak of the EL4 level lies well below the minimum experimental temperature. Figures 7 and 8 show that there remains a small discrepancy in the linewidths of the three-level theory and the DLPTS spectrum with the latter
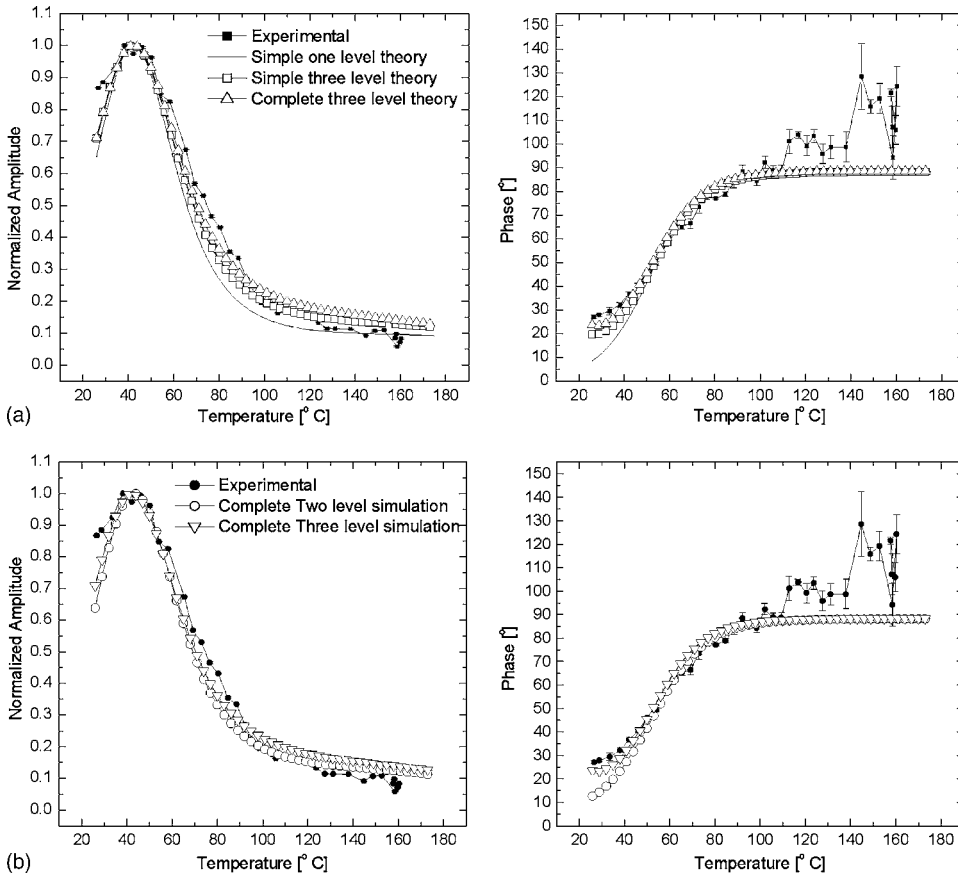
FIG. 7. (a) Experimental and theoretical temperature-scanned DLPTS spectra. Simplified one-level theory, Eqs. (68), (78)–(81), (84), and (85); simplified three-level theory, Eqs. (68), (74)–(77), (84), and (85); and complete three-level theory, Eqs. (72), (73), (84), and (85). (b) Comparison of the theoretical two-level and three-level temperature-scanned DLPTS spectra.

exhibiting slightly more broadening and more complete decay at high temperatures. The effect of carrier diffusion away from the excitation and detection volume is currently under investigation.

Compared with the time-scanned transients, the temperature-scanned photothermal spectrum appears less sensitive to multiple-level effects while it exhibits more significant differences between the simplified and complete theories. Therefore, the complete theory applied to the photothermal temperature spectra can yield optimally correlated energy-level information on the band-gap energy-state distribution in a semiconductor. It is also noted that the complete multiple-level theory yields the best fit to both amplitude and phase photothermal spectra with the exception of the near

baseline temperature range above 100 °C. In conclusion, the combination of the transients and the temperature scan renders the identification of the levels required to satisfy both signals much more robust than that offered by either method individually, as has been the practice to date with DLTS types of measurements.

VI. CONCLUSIONS

A multitrap transport-rate time-gating theory of band-gap trap states in semiconductors with fast band-to-band recombination rate has been presented. The theory exploits the adiabatic character of photoexcitation of nonequilibrium excess free carriers which attains steady-state distribution at
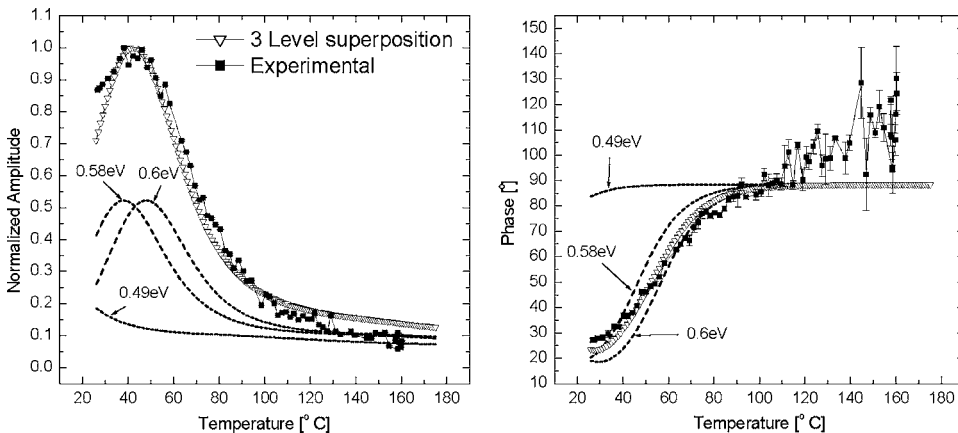
FIG. 8. Temperature-scanned DLPTS spectra superpositions leading to best fit to experimental spectrum.

times very short compared to trap emission and capture effects induced by thermal transport to and from the bandedges of the semiconductor. The theory takes into account contributions to the free-carrier densities, both electrons and holes, from the optical pump as well as from occupied trap states during thermal emission and capture events. It forms the basis of a new two-laser-beam deep level photothermal spectroscopy (DLPTS) which was tested on SI-GaAs. DLPTS was used to fit the experimental temperature-scanned photothermal spectra and the time-resolved transients. Due to the short lifetime and high-resistivity nature of SI-GaAs, the re-trapping of carriers and background free-carrier density can be neglected, which leads to approximately similar fitting results of the time-resolved transient with both complete and simplified theories. However, for a wider application of DLPTS to different semiconductor samples, such as Si, which has much longer lifetime and larger background free-carrier concentration, the introduction of the complete theory in this paper is essential. In fact, the simple theory has already limited the application of other thermal-activation based theories such as PITS, and failed in the explanation of several phenomena including the negative peak in PITS transient.[15] In the fitting of the temperature-scanned spectra, the complete theory yields a higher degree of accuracy. Compared with the simplified one-level approximation used in conventional DLTS, the multitrap theory gave a better fit to all the experimental data, thus yielding accurate information on the energy structure and capture cross sections of the intra-band-gap states participating in the DLPTS signal generation. The combination of time-resolved photothermal responses and temperature-scanned spectra was found to yield optimally accurate information about the types and properties of the energy states, thus setting the stage for an inverse-problem-type of intra-band-gap energy-state spectroscopic reconstructions.

ACKNOWLEDGMENTS

[1] D. V. Lang, J. Appl. Phys. **45**, 3023 (1974).
[2] R. E. Kremer, M. C. Arikan, J. C. Abele, and J. S. Blakemore, J. Appl. Phys. **62**, 2424 (1987).
[3] Ch. Hurtes, M. Boulou, A. Mitonneau, and D. Bois, Appl. Phys. Lett. **32**, 821 (1978).
[4] P. Kaminski and R. Kozlowski, Mater. Sci. Eng., B **B91–B92**, 398 (2002).
[5] H. Oheda, J. Appl. Phys. **52**, 6693 (1981).
[6] G. Schumm and G. Bauer, Phys. Rev. B **39**, 5311 (1989).
[7] C. Longeaud and J. P. Kleider, Phys. Rev. B **45**, 11672 (1992).
[8] C. Longeaud and J. P. Kleider, Phys. Rev. B **48**, 8715 (1993).
[9] P. Kounavis, Phys. Rev. B **64**, 045204 (2001).
[10] J. C. Abele, R. E. Kremer, and J. S. Blakemore, J. Appl. Phys. **62**, 2432 (1987).
[11] Y. Fujisaki, Y. Takano, and T. Ishiba, Jpn. J. Appl. Phys., Part 2 **25**, L874 (1986).
[12] J. Lagowski, P. Edelman, and A. Orawski, Semicond. Sci. Technol. **7**, A211 (1992).
[13] Y. Kirino, A. Buczkowski, Z. J. Radzimski, G. A. Rozgonyi, and F. Shimura, Appl. Phys. Lett. **57**, 2832 (1990).
[14] J. Xia and A. Mandelis, Appl. Phys. Lett. **90**, 062119 (2007).
[15] M. J. S. P. Brasil and P. Motisuke, J. Appl. Phys. **68**, 3370 (1990).
[16] J. K. Rhee and P. K. Bhattacharya, J. Appl. Phys. **53**, 4247 (1982).
[17] O. Yoshie and M. Kamihara, Jpn. J. Appl. Phys., Part 1 **22**, 621 (1983).
[18] P. K. Giri and Y. N. Mohapatra, J. Appl. Phys. **78**, 262 (1995).
[19] W. Shockely and W. T. Read, Jr., Phys. Rev. **87**, 835 (1952).
[20] J. G. Simmons and G. W. Taylor, Phys. Rev. B **4**, 502 (1971).
[21] J. S. Blakemore, *Semiconductor Statistics* (Dover, New York, 1987), Chap. 2.1.
[22] A. S. Jordan, J. Appl. Phys. **51**, 2218 (1980).
[23] K. Seeger, *Semiconductor Physics*, Springer Series on Solid State Science Vol. 40 (Springer-Verlag, New York, 1982).
[24] G. M. Martin, Appl. Phys. Lett. **39**, 747 (1981).
[25] D. S. Day, M. Y. Tsai, B. G. Streetman, and D. V. Lang, J. Appl. Phys. **50**, 5093 (1979).
[26] A. Mandelis, J. Batista, and D. Shaughnessy, Phys. Rev. B **67**, 205208 (2003).
[27] D. C. Look, in *Semiconductors and Semimetals*, edited by R. K. Willardson and A. C. Beer (Academic, New York, 1983), Vol. 19, p. 75.
[28] J. Xia and A. Mandelis (unpublished).
[29] A. Mandelis, Rev. Sci. Instrum. **65**, 3309 (1994).